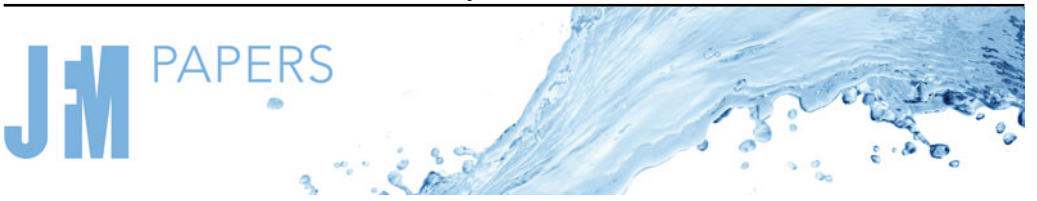
J. Fluid Mech. (2026), *vol.* 1035, A23, doi:10.1017/jfm.2026.11493



An ensemble of Gaussian fields with multifractal statistics for turbulence

Mark Warnecke[1], **Lukas Bentkamp**[2], **Gabriel B. Apolinário**[2], **Michael Wilczek**[2] **and Perry Johnson**[1]

[1]Mechanical & Aerospace Engineering, University of California Irvine, Irvine 92697, USA

[2]Theoretical Physics I, University of Bayreuth, Universitätsstraße 30, Bayreuth 95447, Germany

Corresponding author: Mark Warnecke, mwarneck@uci.edu

(Received 2 September 2025; revised 30 January 2026; accepted 16 March 2026)

Obtaining accurate field statistics continues to be one of the major challenges in turbulence theory and modelling. From the various existing modelling approaches, multifractal models have been successful in capturing intermittency in velocity gradient and increment distributions. Moreover, superstatistical models from non-equilibrium statistical mechanics have shown the capacity to model probability density functions (p.d.f.s) of various statistical turbulent quantities as ensembles of simpler stochastic processes. Here, we present an approach that generates field statistics in the form of a characteristic functional by promoting a model for multifractal increment statistics to an ensemble of Gaussian fields. By carefully designing the correlation function and the corresponding weight of each subensemble, we are able to define a functional that exhibits multifractal two-point inertial-range and dissipation-range statistics, and that blends into realistic large-scale behaviour. Additionally, the method is capable of producing multifractal statistics with any of the widely used singularity spectra. We characterise the fidelity of our approach through comparisons to literature results from direct numerical simulations. Overall, our framework thereby bridges between three different perspectives: superstatistics, multifractals and functional approaches to turbulence.

Key words: isotropic turbulence, intermittency, turbulence theory

1. Introduction

Turbulence is characterised by velocity fluctuations whose statistics are strongly scale-dependent. Probability density functions (p.d.f.s) of the velocity increments are approximately Gaussian at separation distances commensurate to and larger than the integral length scale, but display heavier tails as the separation length scale decreases through the inertial range and into the dissipative range of scales. This phenomenon,

© The Author(s), 2026. Published by Cambridge University Press.

https://doi.org/10.1017/jfm.2026.11493 Published online by Cambridge University Press

known as intermittency, presents a major challenge to creating accurate turbulence models. Over the years, a number of techniques have been developed to model intermittency, such as multifractals and superstatistics, which are reviewed in the following.

In the language of multifractal theory, multiscale observables can be written as a statistical mixture of a continuum of Hölder exponents. Each exponent h occupies a set of dimension $D(h)$ and this determines the contribution of each h to the full statistics (Mandelbrot 1977; Parisi & Frisch 1985; Falconer 1990; Meneveau & Sreenivasan 1991). Among the observables to which multifractal theory has been successfully applied are velocity gradients (Nelkin 1990; Chevillard & Meneveau 2006; Ishihara, Gotoh & Kaneda 2009; Johnson & Meneveau 2017; Pereira *et al.* 2018; Luo, Shi & Meneveau 2022), Eulerian velocity increments (Benzi *et al.* 1984; Meneveau & Sreenivasan 1991), Lagrangian velocity increments (Biferale *et al.* 2004; Chevillard *et al.* 2005, 2012; Arnèodo *et al.* 2008) and Lagrangian acceleration (Biferale *et al.* 2004). Crucially, it provides a connection between the asymptotic scaling of all of these observables in terms of a single $D(h)$ function.

At first glance, superstatistics (Beck & Cohen 2003; Beck 2004, 2011) represents a complementary approach to model intermittency based on a mixture distribution. Applied to non-equilibrium statistical mechanics, superstatistics describes a mixture of Boltzmann statistics with the temperature as the mixing parameter (Beck & Cohen 2003; Beck 2004, 2011). In the context of turbulence, the mixing parameter may be, for instance, the energy dissipation. This description has been shown to capture non-Gaussian turbulence statistics both in the Eulerian (Beck 2000) and Lagrangian frames (Reynolds 2003; Beck 2003, 2007; Reynolds *et al.* 2005). It is also worth noting that the multifractal model can be formulated in a way akin to superstatistics. Specifically, Chevillard *et al.* (2012) considered a superposition of Gaussian increment statistics with a fluctuating variance as a function of the Hölder exponents. Early approaches include those of Castaing, Gagne & Hopfinger (1990), who produced K62 increment statistics as a superposition of Gaussian distributions with a fluctuating variance as a function of the dissipation rate, and Benzi *et al.* (1991), who generated velocity increment and gradient p.d.f.s with anomalous scaling from superpositions based on the random beta model. This indicates that intimate relations between the two approaches exist.

Previous applications of the multifractal and superstatistical approaches have focused on the modelling of individual random variables, e.g. two-point statistics. While the multifractal language provides a connection between the universal properties of different observables (Benzi *et al.* 1991, 1998; Chevillard *et al.* 2012), the interest in extending these approaches to modelling the statistics of entire random fields remains. Wilczek (2016) showed that a superposition of Gaussian characteristic functionals (i.e. a statistical ensemble of Gaussian fields) with a fluctuating correlation function is capable of producing non-Gaussianity and intermittency. This naturally leads to the question whether a mixture model with realistic multifractal properties comprising entire field statistics can be developed. A first step into this direction was recently taken by Friedrich *et al.* (2021), who developed a model for field statistics with classic K62 multifractal scaling (Kolmogorov 1962; Obukhov 1962). The approach has been extended to enable a statistical refinement of sparse data sets by Lübke *et al.* (2023) and has furthermore been applied to the stochastic modelling of turbulent wind fields (Friedrich *et al.* 2022). We mention as well a complementary approach to field statistics, where realisations of a random field are generated with properties compatible with multifractal theory. This can be done with the Gaussian multiplicative chaos, in a static (Chevillard *et al.* 2019) or dynamic approach (Apolinário *et al.* 2022; Beck *et al.* 2024), as well as with multiplicative

https://doi.org/10.1017/jfm.2026.11493 Published online by Cambridge University Press

wavelet decompositions (Benzi, Biferale & Parisi 1993; Arnèodo, Bacry & Muzy 1998) or products of time series (Biferale *et al.* 1998).

In this paper, we establish a relation between existing multifractal models and the superstatistical Gaussian field ensemble approach. We construct an ensemble of Gaussian fields that features increment and gradient statistics complying with a given multifractal singularity spectrum, albeit only for its even moments. This extends previous models based on Gaussian superpositions of two-point velocity increment p.d.f.s to field statistics that contains arbitrary multi-point p.d.f.s via superpositions of Gaussian characteristic functionals. From a conceptual point of view, this highlights close connections between the discussed previous approaches and lays the foundation for a future connection to statistical field theories based on the Navier–Stokes equation such as the functional approach (Hopf 1952; Ohkitani 2020).

The content is arranged as follows. In § 2, we review the multifractal modelling of Chevillard *et al.* (2012) and the ensemble of Gaussian fields of Wilczek (2016). In § 3, we show how the multifractal description can be generalised to a superstatistical characteristic functional. Section 4 demonstrates the approach with a simple example – the classic log-normal model. In § 5, a more general model is considered, with an arbitrary singularity spectrum, and realistic large-scale and viscous-range behaviour. Conclusions are drawn in § 6.

2. Theoretical background

2.1. *Gaussian mixtures for multifractal velocity increment p.d.f.s*

In this section, we summarise the formulation of multifractals as Gaussian mixtures put forward by Chevillard *et al.* (2012). The paper considers velocity increments $v = \delta_\ell u$ across a scale ℓ in the inertial range, i.e. $\eta \ll \ell \ll L$, where η denotes the Kolmogorov scale and L the integral scale of the flow. The velocity increment, conditional on a given Hölder exponent h, is modelled as a zero-mean Gaussian random variable, with p.d.f.

$$g(v;\, S(\ell;\, h)) = \frac{1}{\sqrt{2\pi S(\ell;\, h)}} \exp\left[-\frac{v^2}{2S(\ell;\, h)}\right]. \tag{2.1}$$

Notice that we have adopted a notation for the Gaussian p.d.f. $g(x;\, \sigma^2)$, where σ^2 is the variance. Here, $S(\ell;\, h)$ is the second-order structure function conditional on a given Hölder exponent, and behaves as

$$S(\ell;\, h) = 2\sigma_u^2 \left(1 + \left(\frac{L}{\ell}\right)^2\right)^{-h} \tag{2.2}$$

in the inertial and large-scale ranges. Compared with Chevillard *et al.* (2012), we have added a large-scale saturation. The large-scale root mean square velocity is denoted by σ_u and $S(\ell,\, h)$ correctly asymptotes to $2\sigma_u^2$ as $\ell \to \infty$. Moreover, this function shows an $(\ell/L)^{2h}$ scaling in the inertial range. In this framework, the p.d.f. of velocity increments is given by

$$f_v(v;\, \ell) = \int \mathrm{d}h\; f_h(h;\, \ell)\; g(v;\, S(\ell;\, h)), \tag{2.3}$$

where $f_h(h;\, \ell)$ is the probability density of Hölder exponents at fixed scale ℓ. This mixture of Gaussian random variables with fluctuating variance naturally gives rise to non-Gaussian statistics.

https://doi.org/10.1017/jfm.2026.11493 Published online by Cambridge University Press

In this one-dimensional setting, the mixture distribution $f_h(h;\ell)$ provided by multifractal phenomenology, including the inertial and large-scale ranges, is given by

$$f_h(h;\ell) = \begin{cases} \frac{1}{Z(\ell)}\left(1+(L/\ell)^2\right)^{-(1-D(h))/2} & \text{if } h_{min} \leqslant h \leqslant h_{max}, \\ 0 & \text{otherwise}, \end{cases} \tag{2.4}$$

where $D(h)$ is the multifractal singularity spectrum, h_{min} and h_{max} are bounds on the Hölder exponent (explained later), and $Z(\ell)$ is the normalisation of the p.d.f. A key assumption of the multifractal model, relevant for the subsequent discussion, is that $D(h)$ is assumed to be independent of ℓ over the inertial range of scales.

With this formulation, the velocity increment displays multifractal scaling exponents, at least for its even moments,

$$\langle v^n \rangle \sim \ell^{\zeta_n}, \quad \text{where} \quad \zeta_n = \min_h \left[nh + 1 - D(h)\right], \tag{2.5}$$

as can be shown with a steepest descent approximation in the limit of vanishing scale separation (Chevillard *et al.* 2012). Due to the use of Gaussians, all odd-order moments of the velocity increments are zero. We remark, however, that Chevillard *et al.* (2012) address the skewness of the velocity increments by modifying the Gaussian base distribution.

There are several empirical models for $D(h)$ in the turbulence literature and, in § 3, we consider a change of variables where $D(h)$ can be freely specified. As explicit examples, we consider three representative models of singularity spectra: the log-normal, with a quadratic spectrum

$$D(h) = 1 - \frac{(h-h_0)^2}{2\sigma_h^2}; \tag{2.6}$$

the She–Lévêque model (She & Lévêque 1994), with spectrum

$$D(h) = -1 + 3\left[\frac{1+\log\log\left(\frac{3}{2}\right)}{\log\left(\frac{3}{2}\right)} - 1\right]\left(h-\frac{1}{9}\right) - \frac{3}{\log\left(\frac{3}{2}\right)}\left(h-\frac{1}{9}\right)\log\left(h-\frac{1}{9}\right); \tag{2.7}$$

and the Sreenivasan–Yakhot model (Sreenivasan & Yakhot 2021), defined by

$$D(h) = 1 - c - \beta h + 2\sqrt{c\beta h}. \tag{2.8}$$

The free parameters of the log-normal model can be determined by fits to the statistics of direct numerical simulation (DNS) or experimental data. Typical values are $h_0 = 0.37$, $\sigma_h^2 = 0.025$ (Chevillard *et al.* 2012). For the Sreenivasan–Yakhot model, $\beta = 3c - 3$ and $c = 7.3$ are predicted by Sreenivasan & Yakhot (2021).

The range of Hölder exponents, $h_{min} \leqslant h \leqslant h_{max}$, important for a complete description of the multifractal exponents, requires accurate statistical data at high Reynolds numbers to be reliably inferred. This topic has recently received attention, with numerical simulations done at increasing spatial resolution (Buaria & Pumir 2023) and novel techniques for measuring exponents at negative order (Lashermes *et al.* 2008). Estimates of h_{min} range from -0.88 (Debue *et al.* 2018; Dubrulle 2019) to 0.15 (Lashermes *et al.* 2008). For this study, we rely on simple estimates by choosing h_{min} and h_{max} as the solutions to $D(h) = 0$.

In the remainder of this paper, we introduce a change of variables that allows to map the multifractal framework as outlined earlier to an ensemble of Gaussian fields.

https://doi.org/10.1017/jfm.2026.11493 Published online by Cambridge University Press

2.2. *Ensemble of Gaussian characteristic functionals for non-Gaussian field statistics*

While the statistics of velocity increments (and two-point statistics, more generally) have been a central focus for turbulence theory over the past century, they provide an incomplete characterisation of turbulent fields. A complete description is provided, for instance, by the characteristic functional, satisfying a closed and infinite-dimensional dynamical equation (the Hopf equation, see Hopf 1952; Monin & Yaglom 1971, 1975). This section reviews the approach of Wilczek (2016), where non-Gaussian and intermittent characteristic functionals are built as mixtures (ensembles) of Gaussian random fields (compare also Bentkamp, Lalescu & Wilczek 2019; Friedrich *et al.* 2021, 2022; Lübke *et al.* 2023). While typically not including skewness, this approach provides a simple and analytically tractable basis for capturing the statistics of turbulent fields.

In the following, we consider one-dimensional fields for simplicity. When comparing theoretical results to data from experiments or DNS data, we interpret these fields *cum grano salis* as one-dimensional cuts through three-dimensional fields. An extension of the approach to three-dimensional vector fields is briefly outlined in Appendix B. For a field $u(x)$, the two-point statistics are encapsulated in the following joint p.d.f.:

$$f_2(u_1, u_2) = \langle \delta(u_1 - u(x_1))\delta(u_2 - u(x_2))\rangle, \tag{2.9}$$

or alternatively in its Fourier transform, the two-point characteristic function,

$$\phi_2(\alpha_1, \alpha_2) = \langle \exp\left[\mathrm{i}\,(\alpha_1 u(x_1) + \alpha_2 u(x_2))\right]\rangle. \tag{2.10}$$

Here, the angular brackets denote ensemble averages. Field statistics include the N-point statistics for any number of points N. This can be captured in a single object, the characteristic functional, given by the expression (Hopf 1952; Kolmogorov 1991)

$$\Phi[\alpha] = \left\langle \exp\left[\mathrm{i}\int_{-\infty}^{\infty} \mathrm{d}x\, \alpha(x)u(x)\right]\right\rangle. \tag{2.11}$$

Here, the argument of Φ is the test function $\alpha(x)$. This characteristic functional contains complete information of the probability densities of observing any velocity field configuration $u(x)$. The characteristic functional can be thought of as the functional Fourier transform of the probability measure on the space of velocity fields. While there exist other characterisations of this probability measure, we chose the characteristic functional for its compactness, ease of use, and its connection to the governing equations (Monin & Yaglom 1971, 1975).

In particular, the characteristic functional of a zero-mean Gaussian field $u_\gamma(x)$ is

$$\Phi^G[\alpha; \gamma] = \exp\left[-\frac{1}{2}\int_{-\infty}^{\infty} \mathrm{d}x \int_{-\infty}^{\infty} \mathrm{d}x' \alpha(x)\widetilde{C}(x - x'; \gamma)\alpha(x')\right], \tag{2.12}$$

where $\widetilde{C}(x - x'; \gamma) = \langle u_\gamma(x)u_\gamma(x')\rangle$ denotes the two-point velocity covariance function. Here, we introduced the parameter γ to label a family of Gaussian fields $u_\gamma(x)$, each characterised by its own covariance function $\widetilde{C}(x - x'; \gamma)$. At this stage, we leave the parameter γ unspecified for generality, but examples could be the field's dissipation rate, local Hölder exponent or a function of other parameters; the choice depends on the specific model. We restrict ourselves to statistically homogeneous fields, such that the covariance function is an even function depending only on $x - x'$. Note that the two-point covariance is sufficient to determine the entire field statistics of the Gaussian field. This provides a practical advantage in developing theories based on Gaussian field statistics. Non-Gaussianity may be recovered by superposing the statistics of an ensemble of Gaussian fields (Wilczek 2016). In particular, the covariance function can be chosen

https://doi.org/10.1017/jfm.2026.11493 Published online by Cambridge University Press

to vary depending on a parameter γ, allowing for its interpretation as a conditional covariance function. In this way, the Gaussian fields become subensembles of the full superstatistical model. The characteristic functional for the resulting ensemble statistics thus takes the form

$$\Phi[\alpha] = \int \mathrm{d}\gamma \; f_\gamma(\gamma) \, \Phi^G[\alpha; \gamma], \tag{2.13}$$

where $f_\gamma(\gamma)$ is the p.d.f. of the parameter γ. Note that, by restricting ourselves to zero-mean Gaussian fields, we do not capture odd-order moments. As a result, our model statistics lacks skewness. Chevillard *et al.* (2012) discuss a method to introduce skewness by including correlations between the Hölder exponent h and a unit Gaussian variable δ, which plays a similar role as the Gaussian fields in our formulation. However, this method does not generalise directly to the ensemble of Gaussian fields, which is why we leave the incorporation of skewness for future investigation.

The apparent similarity between (2.3) for expressing multifractal two-point statistics (Chevillard *et al.* 2012) and (2.13) for the superstatistics of random fields invites a closer inspection of the relationship between these two approaches. This is done in the next section and for that, we outline the statistics of velocity increments and gradients that we obtain from the functional description. The velocity increment statistics are obtained by choosing the test function (Monin & Yaglom 1971, 1975; Wilczek 2016)

$$\alpha(x) = \Delta \left[\delta(x - y - \ell) - \delta(x - y)\right], \tag{2.14}$$

which, inserted into (2.13), yields the characteristic function of the increment at scale ℓ

$$\phi_v(\Delta; \ell) = \int \mathrm{d}\gamma \; f_\gamma(\gamma) \; \exp\!\left(-\frac{1}{2}\widetilde{S}(\ell; \gamma)\Delta^2\right), \tag{2.15}$$

with the conditional structure function

$$\widetilde{S}(\ell; \gamma) = 2\left[\widetilde{C}(0; \gamma) - \widetilde{C}(\ell; \gamma)\right]. \tag{2.16}$$

The Fourier transform of this characteristic function produces the increment p.d.f.

$$f_v(v; \ell) = \int \mathrm{d}\gamma \; f_\gamma(\gamma) \, g\left(v; \widetilde{S}(\ell; \gamma)\right). \tag{2.17}$$

Furthermore, the gradient statistics can be found in a similar way, by choosing the test function (Lumley 2007; Wilczek 2016)

$$\alpha(x) = -\beta \frac{\partial}{\partial x}\delta(x - y). \tag{2.18}$$

Using integration by parts before evaluating the delta function, one obtains the characteristic function of the gradient $A = \partial_x u$,

$$\phi_A(\beta) = \int \mathrm{d}\gamma f_\gamma(\gamma) \exp\!\left(\frac{1}{2}\widetilde{C}''(0; \gamma)\beta^2\right) = \int \mathrm{d}\gamma f_\gamma(\gamma) \; \exp\!\left(-\frac{1}{4}\widetilde{S}''(0; \gamma)\beta^2\right), \tag{2.19}$$

where primes denote derivatives with respect to ℓ. A Fourier transform returns the p.d.f. of the velocity gradient,

$$f_A(A) = \int \mathrm{d}\gamma f_\gamma(\gamma) g\left(A; \frac{1}{2}\widetilde{S}''(0; \gamma)\right). \tag{2.20}$$

https://doi.org/10.1017/jfm.2026.11493 Published online by Cambridge University Press

3. Connecting multifractal mixtures and Gaussian ensembles

We may now build a connection between the multifractal formulation of Chevillard *et al.* (2012) and the ensemble of Gaussian fields of Wilczek (2016). Let us start with the multifractal formulation, in particular, (2.3) which we repeat:

$$f_v(v;\,\ell) = \int \mathrm{d}h f_h(h;\,\ell)\; g(v;\,S(\ell;\,h)). \tag{3.1}$$

For this distribution, h is the mixing parameter. However, notice that (2.17), obtained from the ensemble of Gaussians, is also a mixture, this time with the scale-independent mixing distribution f_γ:

$$f_v(v;\,\ell) = \int \mathrm{d}\gamma f_\gamma(\gamma) g\big(v;\,\widetilde{S}(\ell;\,\gamma)\big). \tag{3.2}$$

In (3.1), the scale dependence of f_h is a requirement of multifractal phenomenology, while in (3.2), its absence in f_γ is necessary for the functional formulation. As can be seen in (2.13), the mixing distribution $f_\gamma(\gamma)$ cannot depend on the scale of the observable, which only comes in through the test function (2.14) and thus becomes an argument of the subensemble structure function $\widetilde{S}$. To write an ensemble of Gaussian fields that is compatible with the multifractal formulation of (3.1), we introduce a change of variables which connects γ and h.

Let us introduce the cumulative distribution functions (CDFs)

$$F_h(h;\,\ell) = \int_{-\infty}^{h} \mathrm{d}h' f_h(h';\,\ell) \quad \text{and} \tag{3.3}$$

$$F_\gamma(\gamma) = \int_{-\infty}^{\gamma} \mathrm{d}\gamma' f_\gamma(\gamma')\,. \tag{3.4}$$

We claim that, given the p.d.f.s $f_\gamma(\gamma)$ and $f_h(h;\,\ell)$, as well as a structure function $S(\ell;\,h)$, both superpositions are equivalent, i.e.

$$f_v(v;\,\ell) = \int \mathrm{d}\gamma f_\gamma(\gamma) g\big(v;\,\widetilde{S}(\ell;\,\gamma)\big) = \int \mathrm{d}h\; f_h(h;\,\ell)\; g(v;\,S(\ell;\,h)), \tag{3.5}$$

given that

$$\widetilde{S}(\ell;\,\gamma) = S\Big(\ell;\,F_h^{-1}(F_\gamma(\gamma);\,\ell)\Big). \tag{3.6}$$

To show this, we choose the following ℓ-dependent substitution that maps γ to h:

$$h(\gamma;\,\ell) = F_h^{-1}(F_\gamma(\gamma);\,\ell), \tag{3.7}$$

such that

$$F_h(h(\gamma;\,\ell);\,\ell) = F_\gamma(\gamma). \tag{3.8}$$

A derivative with respect to γ results in

$$\frac{\mathrm{d}}{\mathrm{d}\gamma} F_h(h(\gamma;\,\ell);\,\ell) = \frac{\mathrm{d}F_h(h(\gamma;\,\ell);\,\ell)}{\mathrm{d}h}\frac{\mathrm{d}h}{\mathrm{d}\gamma} = f_h(h;\,\ell)\frac{\mathrm{d}h}{\mathrm{d}\gamma} = \frac{\mathrm{d}F_\gamma(\gamma)}{\mathrm{d}\gamma} = f_\gamma(\gamma), \tag{3.9}$$

and thus the usual change of probability measures

$$f_h(h;\,\ell)\,\mathrm{d}h = f_\gamma(\gamma)\,\mathrm{d}\gamma. \tag{3.10}$$

https://doi.org/10.1017/jfm.2026.11493 Published online by Cambridge University Press

Applying this substitution to the integral, we can write

$$\int \mathrm{d}\gamma f_\gamma(\gamma) g\big(v; \widetilde{S}(\ell;\gamma)\big) = \int \mathrm{d}\gamma f_\gamma(\gamma) g\Big(v; S\Big(\ell; F_h^{-1}(F_\gamma(\gamma);\ell)\Big)\Big) \tag{3.11}$$

$$= \int \mathrm{d}h\; f_h(h;\ell)\, g(v; S(\ell;h)), \tag{3.12}$$

which concludes the argument. This means that the increment statistics from an h ensemble with any scale-dependent p.d.f. f_h can be reproduced by a γ ensemble with a scale-independent p.d.f. f_γ, subject to an appropriate change of the structure function. Note that only the transformed structure function $\widetilde{S}$ is fixed by the transform, whereas the parameter distribution $f_\gamma(\gamma)$ can be chosen freely in advance.

Therefore, we can transform a multifractal model for velocity increment p.d.f.s with arbitrary singularity spectrum into a Gaussian mixture increment p.d.f. with scale-independent mixing distribution. The latter expression can then be generalised to a mixture (ensemble) of characteristic functionals. The resulting functional reproduces the increment statistics of the original multifractal model. Furthermore, it is capable of producing multifractal velocity gradient statistics as well. Chevillard *et al.* (2012), in comparison, constructed velocity gradient statistics through a compatibility argument between random variables at different scales. We illustrate the change of variables (3.7) with various examples in the following sections.

4. Example: log-normal model

As a first example to illustrate the mapping from the multifractal formulation to the ensemble of Gaussian fields, we choose a quadratic singularity spectrum, $D(h) = 1 - ((h-h_0)^2/2\sigma_h^2)$ (2.6), the log-normal multifractal model, without bounds on h ($h_{min} = -\infty$, $h_{max} = \infty$). According to (2.4), the resulting p.d.f. f_h is Gaussian,

$$f_h(h;\ell) = \frac{1}{Z(\ell)} \exp\left[-\log\left(1 + \left(\frac{L}{\ell}\right)^2\right) \frac{(h-h_0)^2}{4\sigma_h^2} \right] = g\big(h - h_0; \Sigma^2(\ell)\big), \tag{4.1}$$

where $Z(\ell)$ is the appropriate normalisation and

$$\Sigma^2(\ell) = \frac{2\sigma_h^2}{\log\Big(1 + \big(\frac{L}{\ell}\big)^2\Big)} \tag{4.2}$$

is the ℓ-dependent variance. Its CDF reads

$$F_h(h;\ell) = \int_{-\infty}^{h} \mathrm{d}h' f_h(h';\ell) = G\left(\frac{h-h_0}{\Sigma(\ell)}\right), \tag{4.3}$$

where $G(x)$ is the CDF of a standard Gaussian. As laid out in the previous section, we want to express the increment p.d.f.s given by (3.1) as a superposition with a scale-independent mixing parameter γ (3.2). Since we can freely choose the distribution of γ, we set it to be a standard Gaussian, with p.d.f. $f_\gamma(\gamma) = g(\gamma;1)$ and CDF $F_\gamma(\gamma) = G(\gamma)$. The mapping is given by (3.7):

$$h(\gamma;\ell) = F_h^{-1}(F_\gamma(\gamma);\ell) = h_0 + \Sigma(\ell) G^{-1}(G(\gamma)) = h_0 + \Sigma(\ell)\gamma\ . \tag{4.4}$$

For the superposition, (3.2), we also need the structure function conditional on γ, $\widetilde{S}$. To this end, we choose the h-dependent structure function $S(\ell, h)$ according to the multifractal

https://doi.org/10.1017/jfm.2026.11493 Published online by Cambridge University Press

formulation (2.2), from which we compute the γ-dependent structure function by (3.6):

$$\begin{aligned}\widetilde{S}(\ell;\gamma) &= S(\ell; h(\gamma;\ell)) \\ &= 2\sigma_u^2\left(1+\left(\frac{L}{\ell}\right)^2\right)^{-h(\gamma;\ell)} \\ &= 2\sigma_u^2\left(1+\left(\frac{L}{\ell}\right)^2\right)^{-h_0-\gamma\sqrt{\frac{2\sigma_h^2}{\log(1+(L/\ell)^2)}}}.\end{aligned} \tag{4.5}$$

Through (2.16), this translates into the γ-dependent covariance function

$$\widetilde{C}(\ell;\gamma) = \sigma_u^2 - \sigma_u^2\left(1+\left(\frac{L}{\ell}\right)^2\right)^{-h_0-\gamma\sqrt{\frac{2\sigma_h^2}{\log(1+(L/\ell)^2)}}}, \tag{4.6}$$

which can be used to construct the full ensemble of Gaussian fields, (2.13). Therefore, we have defined a fully explicit characteristic functional, comprehensively describing field statistics, including log-normal multifractal increment statistics.

While analytically simple, the model allows for arbitrarily negative Hölder exponents, which are unphysical. This issue can be fixed by adding bounds $h_{min} \leqslant h \leqslant h_{max}$, as discussed in § 2.1. The corresponding p.d.f. of Hölder exponents, (2.4), then becomes a truncated Gaussian,

$$f_h(h;\ell) = \begin{cases} \frac{1}{Z(\ell)}\exp\left[-\log\left(1+\left(\frac{L}{\ell}\right)^2\right)\frac{(h-h_0)^2}{4\sigma_h^2}\right] & \text{if } h_{min}\leqslant h\leqslant h_{max}, \\ 0 & \text{otherwise,}\end{cases} \tag{4.7}$$

where $Z(\ell)$ is a new appropriate normalisation. Its CDF is

$$F_h(h;\ell) = \int_{-\infty}^{h} \mathrm{d}h'\, f_h(h';\ell) = \frac{G\left(\frac{h-h_0}{\Sigma(\ell)}\right) - G\left(\frac{h_{min}-h_0}{\Sigma(\ell)}\right)}{G\left(\frac{h_{max}-h_0}{\Sigma(\ell)}\right) - G\left(\frac{h_{min}-h_0}{\Sigma(\ell)}\right)} \quad \text{if } h_{min}\leqslant h\leqslant h_{max}, \tag{4.8}$$

with which we compute a new mapping,

$$h(\gamma;\ell) = F_h^{-1}(F_\gamma(\gamma);\ell) \tag{4.9}$$

$$= h_0 + \Sigma(\ell)\, G^{-1}\left(G\left(\frac{h_{min}-h_0}{\Sigma(\ell)}\right) + G(\gamma)\left(G\left(\frac{h_{max}-h_0}{\Sigma(\ell)}\right) - G\left(\frac{h_{min}-h_0}{\Sigma(\ell)}\right)\right)\right). \tag{4.10}$$

This expression can be used in (4.5) for an improved version of the Gaussian ensemble with log-normal statistics.

Recently, a Gaussian ensemble with log-normal statistics was introduced by Friedrich *et al.* (2021). This approach relies on the combination of a fractional Ornstein–Uhlenbeck process with a rescaling of space depending on a log-normal, scale-independent random parameter. It can be shown that the specific transformation of Friedrich *et al.* (2021) to construct the ensemble of characteristic functionals corresponds to the log-normal case of the general transform method presented here, but with the scale-dependent parameter being the coarse-grained dissipation rate ε_ℓ instead of the Hölder exponent h. More details are provided in Appendix A.

https://doi.org/10.1017/jfm.2026.11493 Published online by Cambridge University Press

5. General multifractal Gaussian ensemble

The mapping (3.7) is applicable to general Hölder exponent p.d.f.s $f_h(h;\ell)$ and structure functions $S(\ell;h)$. In this section, we apply this mapping to a multifractal model with an arbitrary spectrum of exponents. We include bounds for the Hölder exponent, as in the previous section, and add a realistic viscous-range cut-off to the formulation. The main goal of this section is to demonstrate the capacity of the model to reproduce the features of general multifractal models for the increment and gradient statistics of turbulence. For the sake of presentation, we make particular choices for the form of f_h, S and various parameters to be able to evaluate the model numerically and compare with DNS data.

In general, various modelling choices for $S(\ell;h)$ and $f_h(h;\ell)$ are possible as long as they have certain asymptotic scalings in the dissipation, inertial and large-scale ranges. The onset of the dissipation range is built into the multifractal formalism by local Kolmogorov scales $\eta(h) \ll L$ that are functions of the Hölder exponent. They depend on the Reynolds number in the following way (Paladin & Vulpiani 1987; Nelkin 1990; Frisch 1995):

$$\eta(h) = LR^{-\frac{1}{1+h}}, \tag{5.1}$$

where $R = Re/Re_*$, with Re the large-scale Reynolds number and Re_* a tuning coefficient. A general Hölder exponent p.d.f. $f_h(h;\ell)$, for $h_{min} \leqslant h \leqslant h_{max}$, must have the asymptotic scaling:

$$f_h(h;\ell) \sim \begin{cases} \left(\dfrac{\eta(h)}{L}\right)^{1-D(h)} & \text{if } \ell \ll \eta(h), \\ \left(\dfrac{\ell}{L}\right)^{1-D(h)} & \text{if } \eta(h) \ll \ell \ll L, \\ 1 & \text{if } L \ll \ell. \end{cases} \tag{5.2}$$

Additionally, a general $S(\ell;h)$ must have the asymptotic scaling:

$$\frac{S(\ell;h)}{2\sigma_u^2} \sim \begin{cases} \left(\dfrac{\ell}{\eta(h)}\right)^2 \left(\dfrac{\eta(h)}{L}\right)^{2h} & \text{if } \ell \ll \eta(h), \\ \left(\dfrac{\ell}{L}\right)^{2h} & \text{if } \eta(h) \ll \ell \ll L, \\ 1 & \text{if } L \ll \ell. \end{cases} \tag{5.3}$$

Using the general transformation outlined in § 3, any such choice of f_h and S can be used to construct a Gaussian ensemble with multifractal scaling. In the dissipative range, if the conditional structure function, $S(\ell;h)$, matches (5.3), then it shows smooth behaviour for a fixed Hölder exponent. Therefore, the gradient variance of each subensemble is then readily computed as

$$\sigma_A^2 = \lim_{\ell\to 0} \frac{S(\ell;h)}{\ell^2} = 2\frac{\sigma_u^2}{L^2} R^{\frac{2(1-h)}{1+h}}. \tag{5.4}$$

For the subsequent discussion, let us specify particular forms of f_h, S and the distribution of γ. For the conditional structure function, we choose the following extension to (2.2):

$$S(\ell;h) = 2\sigma_u^2 \frac{\left(1+(L/\ell)^2\right)^{-h}}{\left(1+(\eta(h)/\ell)^{2\lambda}\right)^{(1-h)/\lambda}}, \tag{5.5}$$

https://doi.org/10.1017/jfm.2026.11493 Published online by Cambridge University Press

which is essentially how dissipation-range statistics are included by Chevillard *et al.* (2012). This Batchelor interpolation is common in turbulent structure function modelling, for examples, see Arnèodo *et al.* (2008), Chevillard *et al.* (2003), Biferale (2008). The additional parameter λ is a tuning coefficient that controls the onset of the dissipation range. Analogous to (5.5), we also add a viscous-range cut-off to the distribution of Hölder exponents:

$$f_h(h;\,\ell) = \begin{cases} \dfrac{1}{Z(\ell)} \dfrac{\left(1+(\eta(h)/\ell)^{2\lambda}\right)^{(1-D(h))/2\lambda}}{\left(1+(L/\ell)^2\right)^{(1-D(h))/2}} & \text{if } h_{min} \leqslant h \leqslant h_{max}, \\ 0 & \text{otherwise,} \end{cases} \tag{5.6}$$

where $Z(\ell)$ is the normalisation of this p.d.f. The unfixed model parameters Re_* and λ are chosen in § 5.2 by matching our model with the DNS results in figure 3 for the case $n = 2$.

Since the distribution of the scale-independent parameter γ can be freely chosen, for simplicity, we opt here for a uniform distribution between 0 and 1. As a result, the ensemble of functionals (2.13) can be written as

$$\Phi[\alpha] = \int_0^1 \mathrm{d}\gamma\; \Phi_G[\alpha;\,\gamma]. \tag{5.7}$$

Recognising that the CDF of γ is $F_\gamma(\gamma) = \gamma$ (for γ between 0 and 1), (3.8) tells us that γ is equal to the CDF of the Hölder exponent,

$$\gamma(h;\,\ell) = F_h(h;\,\ell) = \int_{-\infty}^{h} \mathrm{d}h'\, f_h(h';\,\ell). \tag{5.8}$$

5.1. *Visualising the transform*

This transform, (5.8), is used to map from the multifractal to the functional formulation, as outlined in § 3. Figure 1 illustrates its behaviour, by showing the structure functions $S(\ell;\,h)$ (panels *a* and *b*), the scale-dependent transform between h and γ (panels *c* and d) and the transformed structure functions $\widetilde{S}(\ell;\,\gamma)$ (panels *e* and f), for the case of the She–Lévêque singularity spectrum. Each column corresponds to a different Reynolds number. The transform (panel *c* and d) is given by the CDF of the Hölder exponents (5.8), which depends on the length scale ℓ. At large scales, the CDF is flatter, corresponding to a broad distribution of h. Due to the large-scale cut-off, the CDFs ultimately converge to a single curve (dark red). At small scales, the CDFs are steeper, corresponding to a narrower h-distribution, also converging to a single curve due to the viscous cut-off (dark blue, mostly hidden). Each value of γ corresponds to a single subensemble in our ensemble of Gaussian fields, but maps to a range of Hölder exponents seen by the different curves for each length scale. At one point in the centre, corresponding to the most likely value of h, the dependence of the transform on the length is weak. For γ-values further away from this centre, the corresponding h-values change with length scale, as visualised by the differently coloured curves.

The upper and lower rows show how the h-dependent structure functions are transformed into the γ-dependent structure functions according to (3.6). This transformation is computed by numerically inverting (5.8). For the larger Reynolds number, the h-dependent structure functions (panel *b*) show clear inertial-range power-law scaling, built into (5.5). The transformed structure functions (panel *f*) are still strongly reminiscent of this, even though their exponents change with length scale (compare with (4.5)).

Another way of looking at our transform is to consider the different h-values that a single γ-value maps to across length scales. This is shown in figure 2 for two different Reynolds

https://doi.org/10.1017/jfm.2026.11493 Published online by Cambridge University Press

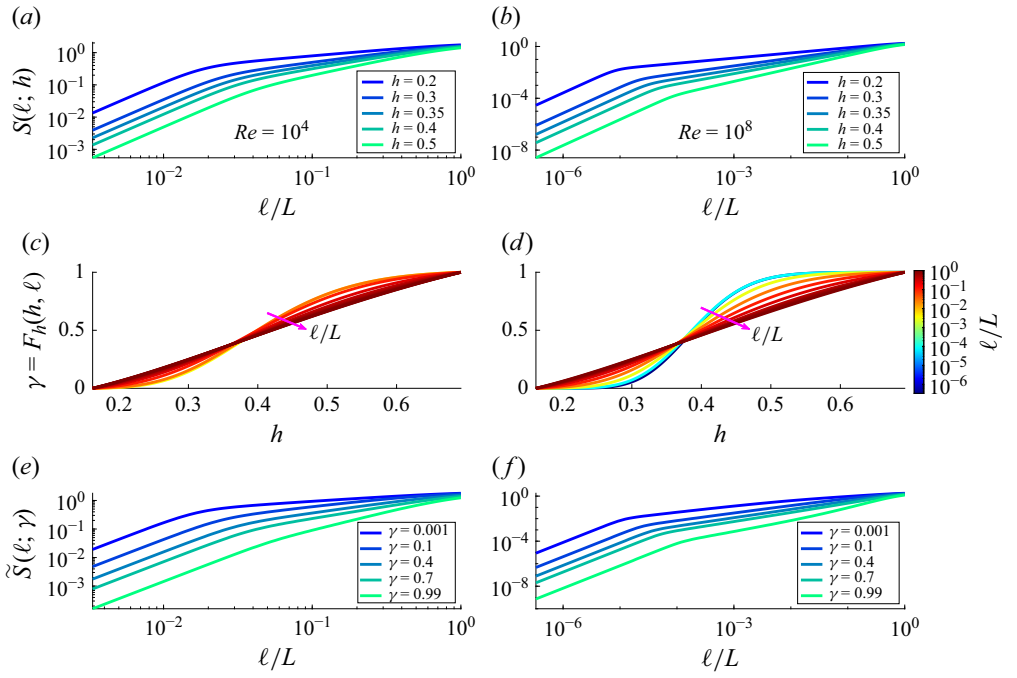


Figure 1. (*a*,*b*) The second-order structure functions at fixed Hölder exponents for (*a*) $Re = 10^4$ and (*b*) $Re = 10^8$. (*c*,*d*) The scale-independent parameter γ plotted versus the Hölder exponent with a magenta arrow indicating the direction of small ℓ to large ℓ. (*e*,*f*) The second-order structure function of selected Gaussian subensembles corresponding to fixed values of γ. For this figure, the Hölder exponent defining the transformation has a She–Lévêque singularity spectrum and varies from 0.162 to 0.694.

numbers. While γ-values around 0.4 correspond to almost constant h-values, other γ-curves cover a wider range of h-values. It is this length dependence in the transform that allows us to encode multifractal statistics using a single distribution for γ (in this case, the uniform distribution between 0 and 1). Figure 2 shows that the variation with ℓ becomes more pronounced as the Reynolds number increases, since the transform has to accommodate very wide (at large scales) and very narrow (at small scales) h-distributions.

5.2. *Increment statistics*

To illustrate how our ensemble of Gaussian fields exhibits multifractal features resembling the statistics of turbulence, we compute increment statistics by numerically evaluating (2.17). Longitudinal absolute-value increment p.d.f.s and structure functions from the model are compared with DNS data in figure 3 (we used the `iso8192` dataset from the Johns Hopkins Turbulence Database (JHTDB), see Li *et al.* 2008 for the database and see Yeung, Zhai & Sreenivasan 2015 for the simulation details). Figure 3(*a*) shows that the model reproduces quantitatively the transition from close-to-Gaussian statistics at large scales to the heavy-tailed distributions characterising the small scales. The corresponding structure functions are shown in figure 3(*b*). Note that these are the unconditional structure functions predicted by the model, not to be confused with the h- and γ-dependent second-order functions $S(\ell; h)$ and $\widetilde{S}(\ell; \gamma)$ used to construct the model. Model parameters in (5.5), (5.6) were chosen to visually fit the $\langle|v|^2\rangle/|\sigma_u|^2$ curve in figure 3(*b*). Their values are $\lambda = 2$, $Re_* = 82$ and $L = 0.67L_D$, where L_D is the integral length scale as reported in the `iso8192` dataset. In figure 3(*b*), we observe a clear power law scaling in the inertial

https://doi.org/10.1017/jfm.2026.11493 Published online by Cambridge University Press

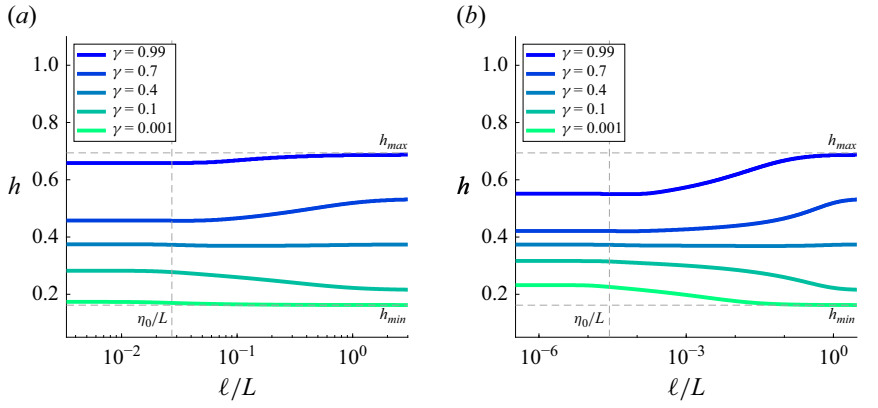


Figure 2. Variation of the Hölder exponent with separation distance of selected members of the ensemble are plotted for Reynolds numbers equal to (*a*) 10^4 and (*b*) 10^8. We define $\eta_0 = \eta(h = 1/3)$ to illustrate the onset of the dissipation range. For this figure, the Hölder exponent defining the transformation has a She–Lévêque singularity spectrum and varies from 0.162 to 0.694.

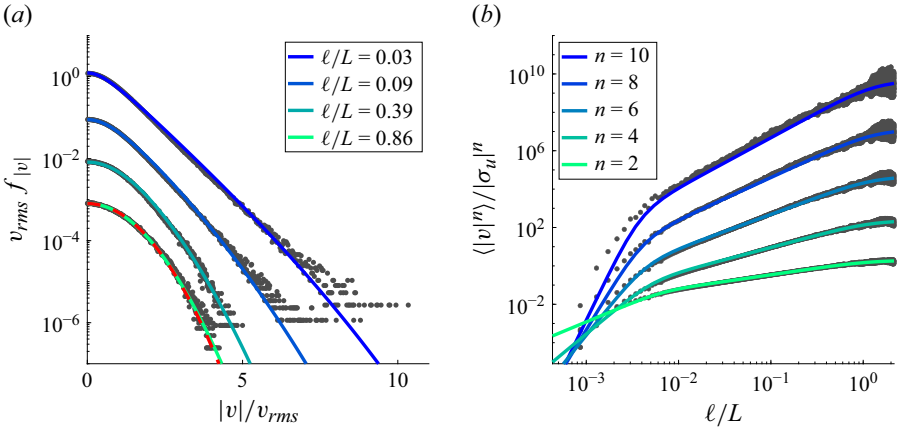


Figure 3. (*a*) The standardised velocity increment p.d.f. at various separation distances from the Gaussian ensemble (lines) plotted against simulation data at $R_\lambda = 1285$ from the JHTDB `iso8192` dataset (points). Additionally a standardised Gaussian is plotted in a red dashed line for reference. (*b*) The nth-order structure function versus separation length (ℓ) from the Gaussian ensemble (lines) plotted against simulation data from the JHTDB `iso8192` dataset (points). For this figure, the Hölder exponent defining the transformation has a She–Lévêque singularity spectrum and varies from 0.162 to 0.694. All curves and points are vertically shifted for clarity.

range matching the DNS data, as well as the proper asymptotic behaviour in the viscous and large scale cut-offs. We add that the exact functional form of the viscous transition may not capture all aspects of its DNS counterpart, but serves as a proof of concept and makes us confident that improved choices of $S(\ell; h)$ and $\widetilde{S}(\ell; \gamma)$ can capture a wide range of features of the data.

By multiplying (2.17) with powers of the increments and integrating analytically, we get

$$\langle v^n \rangle = (n-1)!! \int_0^1 \mathrm{d}\gamma\, \widetilde{S}(\ell; \gamma)^{n/2} \tag{5.9}$$

https://doi.org/10.1017/jfm.2026.11493 Published online by Cambridge University Press

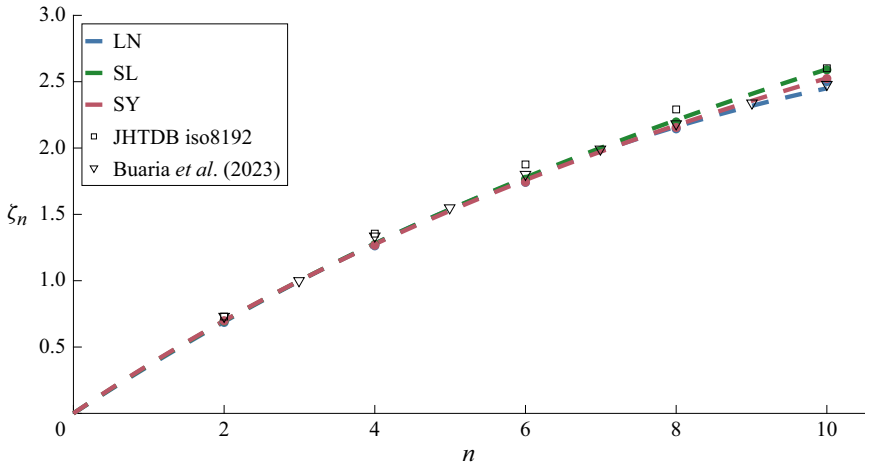


Figure 4. Scaling exponents of the even nth-order structure functions for various singularity spectra – log-normal (LN), She–Lévêque (SL, She & Lévêque 1994) and Sreenivasan–Yakhot (SY, Sreenivasan & Yakhot 2021) – calculated from the Gaussian ensemble (coloured points) and compared with numerical calculations of (2.5), obtained from multifractal theory (colored dashed lines). The minimum and maximum Hölder exponents are set at the points where $D(h) = 0$. Additionally simulation data is plotted from the JHTDB `iso8192` dataset (Li *et al.* 2008; Yeung *et al.* 2015) and Buaria & Sreenivasan (2023).

for even n, which allows us to compute structure functions of any order directly from the second-order subensemble structure functions $\widetilde{S}(\ell;\gamma)$. With our change of variables, (3.7), one can show that the corresponding scaling exponents agree with (2.5). To check this numerically, we measure the scaling of the structure functions in (5.9) in the limit $Re \to \infty$. To this end, we choose an interval of length scales much smaller than L. Then the best linear fit to a double logarithmic plot of (5.9) is used to compute ζ_n. In figure 4, we compare the exponents computed from the model's structure functions (data points) to the exponents expected by the Legendre transform (2.5) (dashed lines), which agree reasonably well. This confirms that the ensemble of Gaussian fields constructed here is capable of reproducing the velocity increment scaling of various multifractal models.

5.3. *Gradient statistics*

Based on the full multi-scale description we introduced at the beginning of § 5, our model is able to predict gradient statistics as well. The tuning parameters (λ, Re_* and L) are set by matching the second-order structure function to data (see § 5.2). The gradient p.d.f., obtained from the functional with the right choice of the test function (2.18), is given by a superposition of Gaussian p.d.f.s, (2.20). The p.d.f. of the absolute value of the gradient is shown at different Reynolds numbers in figure 5(*a*), standardised by its variance, the average of (5.4).

Analogous to the increment moments, gradient moments can be computed by multiplying (2.20) with powers of the gradient and integrating analytically. As a result, gradient moments can be written as

$$\langle A^n \rangle = (n-1)!! \int_0^1 \mathrm{d}\gamma \left(\frac{1}{2} \widetilde{S}''(0;\gamma) \right)^{n/2}. \tag{5.10}$$

https://doi.org/10.1017/jfm.2026.11493 Published online by Cambridge University Press

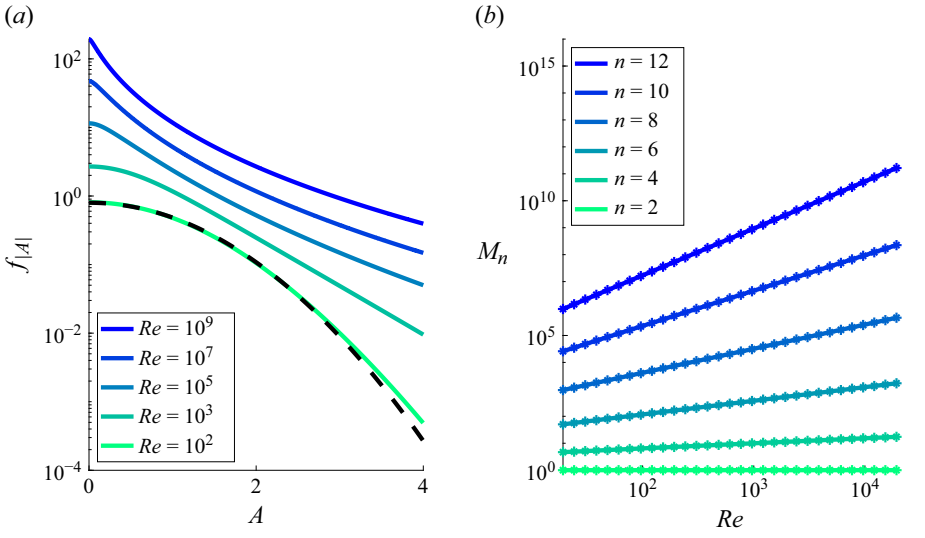


Figure 5. (*a*) Standardised gradient p.d.f.s from the Gaussian ensemble (solid lines), alongside a standardised Gaussian (dashed line) for comparison. (*b*) The nth-order standardised gradient moment from the Gaussian ensemble based on superposition of γ ((5.10), lines) plotted on top of calculations from the corresponding version of (5.10) based on superposition of Hölder exponents (points) versus Reynolds number. The Hölder exponents defining the transformation have a She–Lévêque singularity spectrum and vary from 0.162 to 0.694. The plots are vertically shifted for clarity.

Again, this allows us to compute moments directly from the subensemble structure functions $\widetilde{S}(\ell;\gamma)$. We show the standardised moments,

$$M_n = \frac{\langle A^n \rangle}{\langle A^2 \rangle^{n/2}}, \tag{5.11}$$

as a function of Reynolds number in figure 5(*b*) and compare them with a corresponding calculation made with an ensemble of Hölder exponents to demonstrate the validity of the model. They are expected to scale as a power of the Reynolds number,

$$M_n \sim Re^{\xi_n}. \tag{5.12}$$

To check their scaling, we compute the exponents as linear best fits to the double logarithmic plot in figure 5(*b*). The result is shown in figure 6, and compared with data from a few different DNS and with the exponents obtained from multifractal theory (Nelkin 1990),

$$\rho_n \approx -\min_h \frac{n(h-1)+1-D(h)}{1+h}, \qquad \xi_n = \rho_n - \frac{n}{2}\rho_2. \tag{5.13}$$

The comparison with the expected exponents in figure 6 shows that they agree reasonably well. Again, this confirms that the Gaussian ensemble can reproduce multifractal statistics, also in the case of velocity gradients and their scaling with Reynolds number.

6. Conclusion

The central contribution of this work is that it establishes a connection between multifractal models and functional approaches to turbulence based on ensembles of Gaussian fields. We developed an approach that promotes a multifractal model for increment statistics to a model for entire fields. This is accomplished by a change of variables that transforms

https://doi.org/10.1017/jfm.2026.11493 Published online by Cambridge University Press

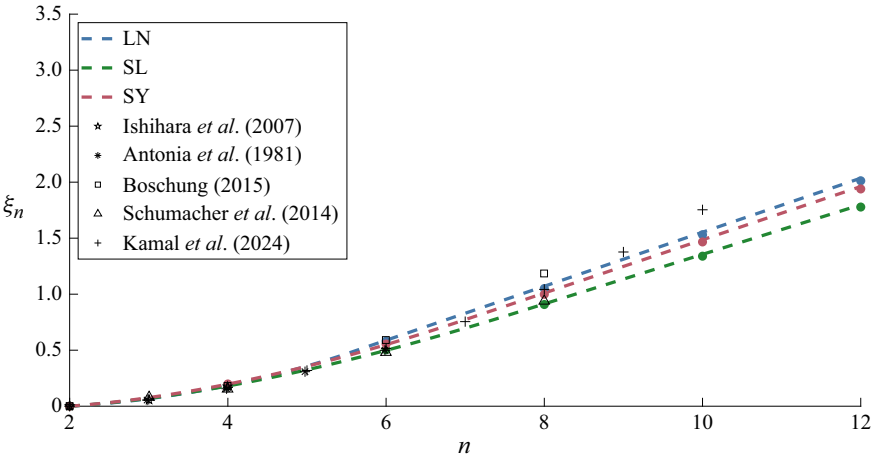


Figure 6. Reynolds number scalings of the standardised velocity gradient moments calculated from the Gaussian ensemble (coloured points) and from (5.13) (dashed curves) for the log-normal (LN), She–Lévêque (SL) and Sreenivasan–Yakhot (SY) singularity spectra. The minimum and maximum Hölder exponents are set at the points where $D(h) = 0$. DNS and experimental results.

a scale-dependent distribution of fluctuating Hölder exponents to a scale-independent distribution over the new parameter γ. This allows for the superposition of Gaussian characteristic functionals parametrised on γ, which then enables the computation of arbitrary field statistics, involving velocity, gradients or increments, for instance.

In the current work, we first demonstrated an analytically tractable instance of the transformation procedure that reproduces velocity increment statistics consistent with the log-normal model. After that, we introduced a more general form of the transformation that can encode multifractal increment and gradient statistics for any singularity spectrum $D(h)$. The resulting characteristic functional can be used to model data from direct numerical simulations (or experiments).

Beyond the present work, the hope is that characteristic functionals, as constructed here, could also be helpful in the context of functional approaches to turbulence such as the Hopf equation (Hopf 1952), which is an elegant way to encode the field statistics of turbulence. A major open question towards this goal is the inclusion of skewness into the current framework, which is crucial to model the effects of self-advection and energy transfer across scales. Another topic for future investigation is the prediction of multiscale correlations of velocity increments (Benzi *et al.* 1998, 1999; Friedrich *et al.* 2018) by the characteristic functional models constructed in this work.

Acknowledgements. We thank Jan Friedrich for helping us to establish the connection of our transform to their work. Additionally, we thank Mostafa Kamal for his simulation data used for the velocity gradient scaling exponent comparisons.

Funding. This project has received funding from the European Research Council (ERC) under the European Union's Horizon 2020 research and innovation programme (Grant agreement No. 101001081).

Declaration of interests. The authors report no conflict of interest.

Appendix A. Connection to the ensemble by Friedrich *et al.* (2021)

In their work on the explicit construction of joint multipoint statistics, Friedrich *et al.* (2021) constructed an ensemble of characteristic functionals exhibiting statistics of the

https://doi.org/10.1017/jfm.2026.11493 Published online by Cambridge University Press

Kolmogorov–Obukhov model (K62; Kolmogorov 1962; Obukhov 1962). The K62 model is formulated in terms of ε_ℓ, the energy dissipation rate coarse-grained over scale ℓ. For simplicity, we focus on the inertial range, $\eta \ll \ell \ll L$, with η the classic Kolmogorov dissipative scale, independent of h. Increment statistics in K62 can be implemented as a superposition of Gaussian distributions (Castaing *et al.* 1990; Friedrich 2025),

$$f_v(v;\ell) = \int \mathrm{d}\varepsilon_\ell \; f_\varepsilon(\varepsilon_\ell;\ell) g(v; S(\ell;\varepsilon_\ell)), \tag{A1}$$

with

$$S(\ell;\varepsilon_\ell) = U^2 \left(\frac{\varepsilon_\ell}{\overline{\varepsilon}}\right)^{2/3} \left(\frac{\ell}{L}\right)^{2/3}. \tag{A2}$$

The distribution of ε_ℓ is assumed to be a scale-dependent log-normal distribution

$$f_\varepsilon(\varepsilon_\ell;\ell) = \frac{1}{\varepsilon_\ell \sqrt{2\pi\sigma^2(\ell)}} \exp\left(-\frac{(\log(\varepsilon_\ell) - M(\ell))^2}{2\sigma^2(\ell)}\right) \tag{A3}$$

with location parameter

$$M(\ell) = \log(\overline{\varepsilon}) - \frac{\sigma^2(\ell)}{2} \tag{A4}$$

and scale parameter

$$\sigma^2(\ell) = \mu \log\left(\frac{L}{\ell}\right). \tag{A5}$$

The K62 model is equivalent to a multifractal model with quadratic singularity spectrum (2.6) and without bounds on h. The difference is that ε_ℓ is used as a fluctuating parameter instead of h. The equivalence can be seen by applying the transformation $\varepsilon_\ell = \overline{\varepsilon}(\ell/L)^{3h-1}$ to (2.2), (2.3) and (2.4), and setting $h_0 = 1/3 + \mu/6$ and $\sigma_h^2 = \mu/9$ while taking the inertial range limit.

With this in mind, we can apply the methodology outlined in § 3 to the K62 model, while replacing each instance of h by ε_ℓ. In contrast to § 4, we choose a unit log-normal distribution for γ, whose CDF is

$$F_\gamma(\gamma) = G(\log(\gamma)). \tag{A6}$$

The CDF of the fluctuating parameter ε_ℓ with scale-dependent p.d.f. (A3) reads

$$F_{\varepsilon_\ell}(\varepsilon_\ell;\ell) = G\left(\frac{\log(\varepsilon_\ell) - M(\ell)}{\sigma(\ell)}\right). \tag{A7}$$

Then, the structure functions of the γ-ensemble can be computed by (3.6) as

$$\widetilde{S}(\ell;\gamma) = S\left(\ell;\, F_{\varepsilon_\ell}^{-1}(F_\gamma(\gamma);\ell)\right) \tag{A8}$$

$$= U^2 \left(\frac{L}{\ell}\right)^{-2/3-\mu/3} \gamma^{\frac{2}{3}\sqrt{\mu \log\left(\frac{L}{\ell}\right)}}. \tag{A9}$$

This turns out to be the same inertial-range form of the structure function as proposed by Friedrich *et al.* (2021). As the basis for their model, they use fractional Ornstein–Uhlenbeck processes with Hölder exponent $H = 1/3$. These are Gaussian processes with a specific, analytically known correlation function. For our considerations, it is only

https://doi.org/10.1017/jfm.2026.11493 Published online by Cambridge University Press

important to know that the corresponding structure function scales as

$$S_{K41}(\ell) \sim \ell^{2H} = \ell^{2/3} \tag{A10}$$

for $\ell \ll L$, which is K41 scaling (Kolmogorov 1941). Then, the subensemble structure functions (A9), which we obtained by application of our method to the K62 model, can also be obtained by applying the following length-scale transform to the K41 structure functions (A10):

$$\ell \to \gamma^{\sqrt{\mu \log\left(\frac{L}{\ell}\right)}} \left(\frac{L}{\ell}\right)^{-\mu/2} \ell. \tag{A11}$$

This is very close to the transform proposed by Friedrich *et al.* (2021, (10)) for a fluctuating parameter $\xi \equiv \gamma$. Overall, this means that the length scale transform proposed by Friedrich *et al.* (2021) can be considered a special case of the more general transform presented here. However, choices regarding the small- and large-scale cut-off were made differently.

We also note that Friedrich *et al.* (2021)'s work and the present framework share the property that a single sample field drawn from the probability distribution will only correspond to a single (random) value of the fluctuating parameter, ξ or γ, respectively. Hence, the full multifractal properties emerge only when averaging over multiple field realisations. To address this, an extension to the work by Friedrich *et al.* (2021) has recently been proposed by Lübke *et al.* (2023), incorporating local fluctuations of the parameter. Adapting our framework in this way would be an interesting future direction to pursue.

Appendix B. Generalisation to vector fields

Our ensemble approach can be straightforwardly generalised to vector fields. To illustrate that, consider a three-dimensional incompressible velocity field $\boldsymbol{u}(\boldsymbol{x})$. Analogous to (2.11) the characteristic functional generalises to

$$\Phi[\boldsymbol{\alpha};\gamma] = \left\langle \exp\left[\mathrm{i}\int_{-\infty}^{\infty} \mathrm{d}\boldsymbol{x}\, \alpha_i(\boldsymbol{x}) u_i(\boldsymbol{x})\right]\right\rangle, \tag{B1}$$

where summation over repeated indices is implied and $\boldsymbol{\alpha}(\boldsymbol{x})$ is a three-dimensional test function. If $\boldsymbol{u}(\boldsymbol{x})$ is an incompressible statistically homogeneous Gaussian vector field with zero mean, its characteristic functional takes the form

$$\Phi^G[\boldsymbol{\alpha}] = \exp\left[-\frac{1}{2}\int_{-\infty}^{\infty} \mathrm{d}\boldsymbol{x} \int_{-\infty}^{\infty} \mathrm{d}\boldsymbol{x}' \alpha_i(\boldsymbol{x}) \widetilde{C}_{ij}(\boldsymbol{x}-\boldsymbol{x}';\gamma)\alpha_j(\boldsymbol{x}')\right], \tag{B2}$$

analogous to (2.12). Assuming statistical isotropy and incompressibility, the covariance tensor $\widetilde{C}_{ij}(\boldsymbol{x}-\boldsymbol{x}';\gamma) = \langle u_i(\boldsymbol{x}) u_j(\boldsymbol{x}')\rangle$ can be written as (Pope 2000)

$$\widetilde{C}_{ij}(\boldsymbol{r};\gamma) = \sigma_u^2 \left(\left[\tilde{f}(r;\gamma) + \frac{1}{2} r \tilde{f}'(r;\gamma)\right]\delta_{ij} - \frac{1}{2} r \tilde{f}'(r;\gamma)\, \hat{r}_i \hat{r}_j\right), \tag{B3}$$

where $\tilde{f}(r;\gamma)$ is the longitudinal velocity autocorrelation function, prime indicates a derivative with respect to r; $\hat{\boldsymbol{r}}$ denotes the unit vector in the direction of $\boldsymbol{r}$.

As a next step, we can relate the longitudinal autocorrelation function to the conditional structure function

$$\tilde{f}(r;\gamma) = 1 - \frac{1}{2\sigma_u^2}\tilde{S}(r;\gamma), \tag{B4}$$

https://doi.org/10.1017/jfm.2026.11493 Published online by Cambridge University Press

which then allows to establish the relationship between a multifractal model for the increment p.d.f.s as outlined in § 3. Once the covariance tensor is determined this way, the Gaussian ensemble (2.13) straightforwardly generalises.

Quite obviously, addressing the question of how to include skewness into this framework is even more relevant for the generalisation to vectorial statistics. This is, however, beyond the scope of the current work.

References

Antonia, R.A., Chambers, A.J. & Satyaprakash, B.R. 1981 Reynolds number dependence of high-order moments of the streamwise turbulent velocity derivative. *Boundary-Layer Meteorol.* **21**, 159–171.

Apolinário, G.B., Chevillard, L. & Mourrat, J.-C. 2022 Dynamical fractional and multifractal fields. *J. Stat. Phys.* **186** (1), 15.

Arnèodo, A. *et al.* 2008 Universal intermittent properties of particle trajectories in highly turbulent flows. *Phys. Rev. Lett.* **100**, 254504.

Arnèodo, A., Bacry, E. & Muzy, J.F. 1998 Random cascades on wavelet dyadic trees. *J. Math. Phys.* **39** (8), 4142–4164.

Beck, C. 2000 Application of generalized thermostatistics to fully developed turbulence. *Phys. A: Stat. Mech. Applics* **277** (1), 115–123.

Beck, C. 2003 Lagrangian acceleration statistics in turbulent flows. *Europhys. Lett.* **64** (2), 151.

Beck, C. 2004 Superstatistics: theory and applications. *Contin. Mech. Thermodyn.* **16**, 293–304.

Beck, C. 2007 Statistics of three-dimensional lagrangian turbulence. *Phys. Rev. Lett.* **98**, 064502.

Beck, C. 2011 Generalized statistical mechanics for superstatistical systems. *Phil. Trans. R. Soc. A: Math. Phys. Engng Sci.* **369** (1935), 453–465.

Beck, C. & Cohen, E.G.D. 2003 Superstatistics. *Phys. A: Stat. Mech. Applics* **322**, 267–275.

Beck, G., Bréhier, C.-E., Chevillard, L., Grande, R. & Ruffenach, W. 2024 Numerical simulations of a stochastic dynamics leading to cascades and loss of regularity: Applications to fluid turbulence and generation of fractional Gaussian fields. *Phys. Rev. Res.* **6** (3), 033048.

Bentkamp, L., Lalescu, C.C. & Wilczek, M. 2019 Persistent accelerations disentangle Lagrangian turbulence. *Nat. Commun.* **10** (1), 3550.

Benzi, R., Biferale, L., Paladin, G., Vulpiani, A. & Vergassola, M. 1991 Multifractality in the statistics of the velocity gradients in turbulence. *Phys. Rev. Lett.* **67**, 2299–2302.

Benzi, R., Biferale, L. & Parisi, G. 1993 On intermittency in a cascade model for turbulence. *Phys. D: Nonlinear Phenom.* **65** (1), 163–171.

Benzi, R., Biferale, L., Ruiz-Chavarria, G., Ciliberto, S. & Toschi, F. 1999 Multiscale velocity correlation in turbulence: experiments, numerical simulations, synthetic signals. *Phys. Fluids* **11** (8), 2215–2224.

Benzi, R., Biferale, L. & Toschi, F. 1998 Multiscale velocity correlations in turbulence. *Phys. Rev. Lett.* **80** (15), 3244.

Benzi, R., Paladin, G., Parisi, G. & Vulpiani, A. 1984 On the multifractal nature of fully developed turbulence and chaotic systems. *J. Phys. A: Math. Gen.* **17** (18), 3521–3531.

Biferale, L. 2008 A note on the fluctuation of dissipative scale in turbulence. *Phys. Fluids* **20** (3), 031703.

Biferale, L., Boffetta, G., Celani, A., Crisanti, A. & Vulpiani, A. 1998 Mimicking a turbulent signal: sequential multiaffine processes. *Phys. Rev. E* **57** (6), R6261.

Biferale, L., Boffetta, G., Celani, A., Devenish, B.J., Lanotte, A. & Toschi, F. 2004 Multifractal statistics of Lagrangian velocity and acceleration in turbulence. *Phys. Rev. Lett.* **93**, 064502.

Boschung, J. 2015 Exact relations between the moments of dissipation and longitudinal velocity derivatives in turbulent flows. *Phys. Rev. E* **92**, 043013.

Buaria, D. & Pumir, A. 2023 Role of pressure in the dynamics of intense velocity gradients in turbulent flows. *J. Fluid Mech.* **973**, A23.

Buaria, D. & Sreenivasan, K.R. 2023 Saturation and multifractality of Lagrangian and Eulerian scaling exponents in three-dimensional turbulence. *Phys. Rev. Lett.* **131**, 204001.

Castaing, B., Gagne, Y. & Hopfinger, E.J. 1990 Velocity probability density functions of high Reynolds number turbulence. *Phys. D: Nonlinear Phenom.* **46** (2), 177–200.

Chevillard, L., Castaing, B., Arnèodo, A., Lévêque, E., Pinton, J.-F. & Roux, S.G. 2012 A phenomenological theory of Eulerian and Lagrangian velocity fluctuations in turbulent flows. *C. R. Phys.* **13** (9–10), 899–928.

https://doi.org/10.1017/jfm.2026.11493 Published online by Cambridge University Press

CHEVILLARD, L., GARBAN, C., RHODES, R. & VARGAS, V. 2019 On a skewed and multifractal unidimensional random field, as a probabilistic representation of Kolmogorov's views on turbulence. *Ann. Henri Poincaré* **20**, 3693–3741.

CHEVILLARD, L. & MENEVEAU, C. 2006 Lagrangian dynamics and statistical geometric structure of turbulence. *Phys. Rev. Lett.* **97**, 174501.

CHEVILLARD, L., ROUX, S.G., LEVÊQUE, E., MORDANT, N., PINTON, J.-F. & ARNÈODO, A. 2003 Lagrangian velocity statistics in turbulent flows: effects of dissipation. *Phys. Rev. Lett.* **91**, 214502.

CHEVILLARD, L., ROUX, S.G., LÉVÊQUE, E., MORDANT, N., PINTON, J.-F. & ARNÈODO, A. 2005 Intermittency of velocity time increments in turbulence. *Phys. Rev. Lett.* **95**, 064501.

DEBUE, P., SHUKLA, V., KUZZAY, D., FARANDA, D., SAW, E.-W., DAVIAUD, F. & DUBRULLE, B. 2018 Dissipation, intermittency, and singularities in incompressible turbulent flows. *Phys. Rev. E* **97** (5), 053101.

DUBRULLE, B. 2019 Beyond Kolmogorov cascades. *J. Fluid Mech.* **867**, P1.

FALCONER, K. 1990 *Fractal Geometry: Mathematical Foundations and Applications*. Wiley.

FRIEDRICH, J. 2025 Joint statistics of complex systems. Habilitation thesis, Universität Oldenburg, Germany.

FRIEDRICH, J., MARGAZOGLOU, G., BIFERALE, L. & GRAUER, R. 2018 Multiscale velocity correlations in turbulence and Burgers turbulence: fusion rules, Markov processes in scale, and multifractal predictions. *Phys. Rev. E* **98** (2), 023104.

FRIEDRICH, J., MORENO, D., SINHUBER, M., WÄCHTER, M. & PEINKE, J. 2022 Superstatistical wind fields from pointwise atmospheric turbulence measurements. *PRX Energy* **1** (2), 023006.

FRIEDRICH, J., PEINKE, J., PUMIR, A. & GRAUER, R. 2021 Explicit construction of joint multipoint statistics in complex systems. *J. Phys.: Complexity* **2** (4), 045006.

FRISCH, U. 1995 *Turbulence: The Legacy of A. N. Kolmogorov*. Cambridge University Press.

HOPF, E. 1952 Statistical hydromechanics and functional calculus. *J. Rat. Mech. Anal.* **1**, 87–123.

ISHIHARA, T., GOTOH, T. & KANEDA, Y. 2009 Study of high–Reynolds number isotropic turbulence by direct numerical simulation. *Annu. Rev. Fluid Mech.* **41**, 165–180.

ISHIHARA, T., KANEDA, M., YOKOKAWA, K., ITAKURA, K. & UNO, A. 2007 Small-scale statistics in high-resolution direct numerical simulation of turbulence: Reynolds number dependence of one point. *J. Fluid Mech.* **592**, 335–366.

JOHNSON, P.L. & MENEVEAU, C. 2017 Turbulence intermittency in a multiple-time-scale Navier–Stokes-based reduced model. *Phys. Rev. Fluids* **2**, 072601.

KAMAL, M. & JOHNSON, P.L. 2024 Artificial bottleneck effect in large eddy simulations. *Phys. Rev. Fluids* **9**, 084605.

KOLMOGOROV, A.N. 1941 The local structure of turbulence in incompressible viscous fluid for very large Reynolds numbers. *C. R. Acad. Sci. URSS* **30**, 301–305.

KOLMOGOROV, A.N. 1962 A refinement of previous hypotheses concerning the local structure of turbulence in a viscous incompressible fluid at high Reynolds number. *J. Fluid Mech.* **13** (1), 82–85.

KOLMOGOROV, A.N. 1991 Laplace transformation in linear spaces. In *Selected Works of A. N. Kolmogorov I: Mathematics and Mechanics* (ed. V.M. Tikhomirov), pp. 194–195. Springer Dordrecht. Originally published in C. R. Acad. Sci. Paris, 200 (1935), 1717–1718.

LASHERMES, B., ROUX, S.G., ABRY, P. & JAFFARD, S. 2008 Comprehensive multifractal analysis of turbulent velocity using the wavelet leaders. *Eur. Phys. J. B* **61**, 201–215.

LI, Y., PERLMAN, E., WAN, M., YANG, Y., MENEVEAU, C., BURNS, R., CHEN, S., SZALAY, A. & EYINK, G. 2008 A public turbulence database cluster and applications to study Lagrangian evolution of velocity increments in turbulence. *J. Turbul.* **9** (31), 1–29.

LÜBKE, J., FRIEDRICH, J. & GRAUER, R. 2023 Stochastic interpolation of sparsely sampled time series by a superstatistical random process and its synthesis in Fourier and wavelet space. *J. Phys.: Complexity* **4** (1), 015005.

LUMLEY, J.L. 2007 *Stochastic Tools in Turbulence*. Dover Publications.

LUO, Y., SHI, Y. & MENEVEAU, C. 2022 Multifractality in a nested velocity gradient model for intermittent turbulence. *Phys. Rev. Fluids* **7**, 014609.

MANDELBROT, B. 1977 *Fractals: Form, Chance and Dimension*. W. H. Freeman and Co.

MENEVEAU, C. & SREENIVASAN, K.R. 1991 The multifractal nature of turbulent energy dissipation. *J. Fluid Mech.* **224**, 429–484.

MONIN, A.S. & YAGLOM, A.M. 1971 *Statistical Fluid Mechanics*, vol. I. MIT Press.

MONIN, A.S. & YAGLOM, A.M. 1975 *Statistical Fluid Mechanics*, vol. II. MIT Press.

NELKIN, M. 1990 Multifractal scaling of velocity derivatives in turbulence. *Phys. Rev. A* **42** (12), 7226–7229.

OBUKHOV, A.M. 1962 Some specific features of atmospheric turbulence. *J. Geophys. Res.* **67** (8), 3011–3014.

OHKITANI, K. 2020 Study of the Hopf functional equation for turbulence: Duhamel principle and dynamical scaling. *Phys. Rev. E* **101** (1), 013104.

https://doi.org/10.1017/jfm.2026.11493 Published online by Cambridge University Press

PALADIN, G. & VULPIANI, A. 1987 Degrees of freedom of turbulence. *Phys. Rev. A* **35** (4), 1971–1973.
PARISI, G. & FRISCH, U. 1985 On the singularity structure of fully developed turbulence. *Turbul. Predictability Geophys. Fluid Dyn. Clim. Dyn.* **88**, 84–88.
PEREIRA, F.S., EÇA, L., VAZ, G. & GIRIMAJI, S.S. 2018 Challenges in scale-resolving simulations of turbulent wake flows with coherent structures. *J. Comput. Phys.* **363**, 98–115.
POPE, S.B. 2000 *Turbulent Flows*. Cambridge University Press.
REYNOLDS, A.M. 2003 Superstatistical mechanics of tracer-particle motions in turbulence. *Phys. Rev. Lett.* **91**, 084503.
REYNOLDS, A.M., MORDANT, N., CRAWFORD, A.M. & BODENSCHATZ, E. 2005 On the distribution of Lagrangian accelerations in turbulent flows. *New J. Phys.* **7** (1), 58.
SCHUMACHER, J., SCHEEL, J.D., KRASNOV, D., DONZIS, D.A., YAKHOT, V. & SREENIVASAN, K.R. 2014 Small-scale universality in fluid turbulence. *Proc. Natl Acad. Sci. USA* **111** (30), 10961–10965.
SHE, Z.-S. & LÉVÊQUE, E. 1994 Universal scaling laws in fully developed turbulence. *Phys. Rev. Lett.* **72**, 336–339.
SREENIVASAN, K.R. & YAKHOT, V. 2021 Dynamics of three-dimensional turbulence from Navier–Stokes equations. *Phys. Rev. Fluids* **6**, 104604.
WILCZEK, M. 2016 Non-Gaussianity and intermittency in an ensemble of Gaussian fields. *New J. Phys.* **18** (12), 125009.
YEUNG, P.K., ZHAI, X.M. & SREENIVASAN, K.R. 2015 Extreme events in computational turbulence. *Proc. Natl Acad. Sci. USA* **112** (41), 12633–12638.

https://doi.org/10.1017/jfm.2026.11493 Published online by Cambridge University Press